Journal of Chemical and Engineering Data, Vol. 24, No. 2, 1979 **133**

Excess Thermodynamic Functions for Ternary Systems. 5. Total-Pressure Data and G^E for 1,4-Dioxane–Ethanol–Water at 50 °C

A. Mario Balcâzar-Ortiz, Rohit B. Patel, Michael M. Abbott,* and Hendrick C. Van Ness*

Chemical and Environmental Engineering Department, Rensselaer Polytechnic Institute, Troy, New York 12181

Isothermal $P-x$ data for the ternary system 1,4-dioxane–ethanol–water at 50 °C are reported, together with data for the constituent binaries. Data reduction by Barker's method provides a correlation for G^E.

The data set reported here comprises VLE measurements for the system 1,4-dioxane (1)–ethanol (2)–water (3) at 50 °C. Experimental values of total vapor pressure as a function of liquid composition are presented for the three constituent binaries and for three runs on ternary mixtures formed by additions of each pure constituent to equimolar mixtures of the other two. The apparatus is that of Gibbs and Van Ness (*6*) as modified by DiElsi et al. (*5*).

The dioxane was chromatoquality reagent from Matheson Coleman and Bell; the reagent-grade ethanol was supplied by U.S. Industrial Chemicals, and the water was doubly deionized. Except for degassing, all reagents were used as received, with indicated purities of at least 99.8 mol %. Vapor pressures of the pure constituents measured in this work and comparable values from the literature are reported in Table I. The P_i^{sat} values in all calculations are fixed at averages of our experimental measurements.

Table I. Vapor Pressures of Pure Constituents at 50 °C in kPa

	1,4-dioxane (1)	ethanol (2)	water (3)
present work	15.709	29.479	12.344
	15.701	29.467	12.347
	15.707	29.471	12.355
			12.342
av value	15.706	29.472	12.347
lit. values	15.908 (*13*)	29.494 (*4*)	12.345 (*3, 10*)
	16.064 (*12*)	29.481 (*10*)	12.349 (*7*)
	15.785 (*9*)	29.493 (*14*)	12.350 (*14*)

Table II. Total Pressure Data for Dioxane (1)-Ethanol (2) at 50 °C

x_1	x_2	P, kPa	P, mmHg
0.0	1.0000	29.479	221.11
0.0261	0.9739	29.839	223.81
0.0755	0.9245	30.254	226.92
0.1305	0.8695	30.451	228.40
0.1977	0.8023	30.456	228.44
0.2765	0.7235	30.323	227.44
0.3587	0.6413	29.844	223.85
0.3909	0.6091	29.572	221.81
0.4330	0.5670	29.275	219.58
0.4670	0.5330	28.960	217.22
0.5095	0.4905	28.574	214.32
0.5474	0.4526	28.114	210.87
0.5666	0.4334	27.882	209.13
0.6212	0.3788	27.128	203.48
0.7071	0.2929	25.547	192.37
0.7742	0.2258	24.210	181.59
0.8535	0.1465	21.964	164.74
0.9311	0.0689	19.073	143.06
0.9690	0.0310	17.515	131.37
1.0000	0.0	15.709	117.83

Table III. Total Pressure Data for Dioxane (1)-Water (2) at 50 °C

x_1	x_2	P, kPa	P, mmHg
0.0	1.0000	12.344	92.59
0.0310	0.9690	15.051	112.89
0.0732	0.9268	17.489	131.18
0.1044	0.8956	18.690	140.19
0.1362	0.8638	19.596	146.98
0.1951	0.8049	20.668	155.02
0.2687	0.7313	21.396	160.48
0.3402	0.6598	21.737	163.04
0.3675	0.6325	21.834	163.77
0.3924	0.6076	21.884	164.14
0.4385	0.5615	21.993	164.96
0.4928	0.5072	22.002	165.03
0.5022	0.4978	22.066	165.51
0.5582	0.4418	22.086	165.66
0.6312	0.3688	22.086	165.66
0.7114	0.2886	21.974	164.82
0.8605	0.1395	20.708	155.32
0.9275	0.0725	19.146	143.61
0.9815	0.0185	16.812	126.10
1.0000	0.0	15.701	117.77

Table IV. Total Pressure Data for Ethanol (1)-Water (2) at 50 °C

x_1	x_2	P, kPa	P, mmHg
0.0	1.0000	12.355	92.67
0.0	1.0000	12.347	92.61
0.0253	0.9747	15.633	117.26
0.0280	0.9720	15.899	119.25
0.0536	0.9464	18.228	136.72
0.0820	0.9180	20.276	152.08
0.0878	0.9122	20.594	154.47
0.1398	0.8602	22.822	171.18
0.1518	0.8482	23.171	173.80
0.2297	0.7703	24.779	185.86
0.2430	0.7570	24.930	186.99
0.3442	0.6558	26.190	196.44
0.3482	0.6518	26.169	196.28
0.3570	0.6430	26.263	196.99
0.3960	0.6040	26.604	199.55
0.4526	0.5474	27.172	203.81
0.4609	0.5391	27.144	203.60
0.5610	0.4390	28.018	210.15
0.5680	0.4320	27.979	209.86
0.5917	0.4083	28.187	211.42
0.6528	0.3472	28.600	214.52
0.7297	0.2703	29.002	217.53
0.8412	0.1588	29.402	220.53
0.8950	0.1050	29.483	221.14
0.9469	0.0531	29.515	221.38
1.0000	0.0	29.467	221.02

Results and Correlations

Tables II through IV give experimental values of total pressures for the three constituent binaries, and Table V contains all data for the three runs made with ternary mixtures. Data reduction is by Barker's method according to procedures described earlier (*1*, *2*). For all three binary systems the analytical expression for G^E is provided by the three-parameter Margules equation

$$g_{ij} \equiv G^E_{ij}/RT = [A_{ji}x_i + A_{ij}x_j - \lambda x_i x_j]x_i x_j \qquad (1)$$

0021-9568/79/1724-0133$01.00/0

Table V. Total Pressure Data for Dioxane (1)-Ethanol (2)-Water (3) at 50 °C

x_1	x_2	x_3	P, kPa	P, mmHg
0.0	0.0	1.0000	12.342	92.57
0.4842	0.0	0.5158	22.056	165.43
0.4731	0.0229	0.5040	22.627	169.72
0.4611	0.0477	0.4912	23.161	173.72
0.4342	0.1032	0.4626	24.289	182.18
0.4132	0.1466	0.4402	25.038	187.80
0.3884	0.1979	0.4137	25.853	193.91
0.3665	0.2430	0.3905	26.476	198.59
0.3414	0.2949	0.3637	27.106	203.31
0.3180	0.3432	0.3388	27.708	207.83
0.2952	0.3903	0.3145	28.127	210.97
0.2706	0.4412	0.2882	28.558	214.20
0.0	1.0000	0.0	29.471	221.05
0.0	0.4983	0.5017	27.554	206.67
0.0264	0.4851	0.4885	27.651	207.40
0.0511	0.4728	0.4761	27.730	207.99
0.1056	0.4457	0.4487	27.912	209.36
0.1550	0.4211	0.4239	27.942	209.58
0.2056	0.3959	0.3985	27.899	209.26
0.2567	0.3705	0.3728	27.784	208.40
0.3063	0.3457	0.3480	27.634	207.27
0.3543	0.3219	0.3238	27.434	205.77
0.4040	0.2971	0.2989	27.144	203.60
1.0000	0.0	0.0	15.707	117.81
0.5012	0.4988	0.0	28.627	214.72
0.4859	0.4836	0.0305	28.638	214.80
0.4692	0.4670	0.0638	28.615	214.63
0.4476	0.4454	0.1070	28.540	214.07
0.4262	0.4242	0.1496	28.415	213.13
0.4011	0.3992	0.1997	28.250	211.89
0.3738	0.3720	0.2542	28.003	210.04
0.3504	0.3488	0.3008	27.726	207.96
0.2740	0.2727	0.4533	26.795	200.98

Table VI. Summary of Results for Binary Systems at 50 °C[a]

	1,4-dioxane (1)-ethanol (2)	1,4-dioxane (1)-water (3)	ethanol (2)-water (3)
P_i^{sat}, kPa	15.706	15.706	29.472
P_j^{sat}, kPa	29.472	12.347	12.347
V_i^L, cm³/mol	88.13	88.13	60.36
V_j^L, cm³/mol	60.36	18.23	18.23
B_{ii}, cm³/mol	−1632	−1632	−1706
B_{jj}, cm³/mol	−1706	−1674	−1674
B_{ij}, cm³/mol	−1016	−318	−948
A_{ij}	1.059 ± 0.009	1.986 ± 0.008	1.708 ± 0.008
A_{ji}	0.920 ± 0.011	1.923 ± 0.006	0.960 ± 0.005
λ	0.232 ± 0.036	0.553 ± 0.025	0.396 ± 0.023
RMS ΔP, kPa	0.040	0.027	0.041
max $\lvert\Delta P\rvert$, kPa	0.141	0.075	0.081
x_i^{az}	0.1656	0.5673	0.9288
P^{az}, kPa	30.508	22.086	29.562

[a] Pairs of components are listed in the order i,j.

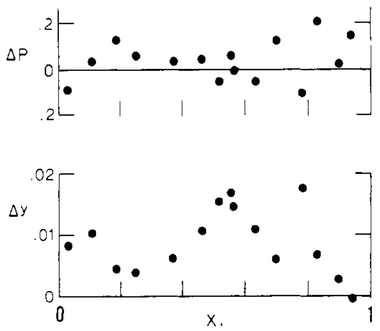

Figure 1. Comparison of the P-x-y data of Valent (12) with the correlation of this work for 1,4-dioxane (1)-water at 50 °C. The pressure residuals ΔP(kPa) and vapor composition residuals Δy_1 are differences between values from this work and those of Valent.

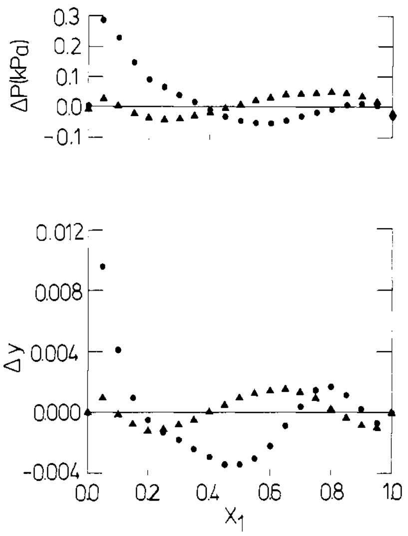

Figure 2. Comparison of correlated results from this work with correlated results of Larkin and Pemberton (8) and of Wilson et al. (14) for ethanol (1)-water at 50 °C. The residuals ΔP and Δy_1 are differences between values from this work and those from the literature.

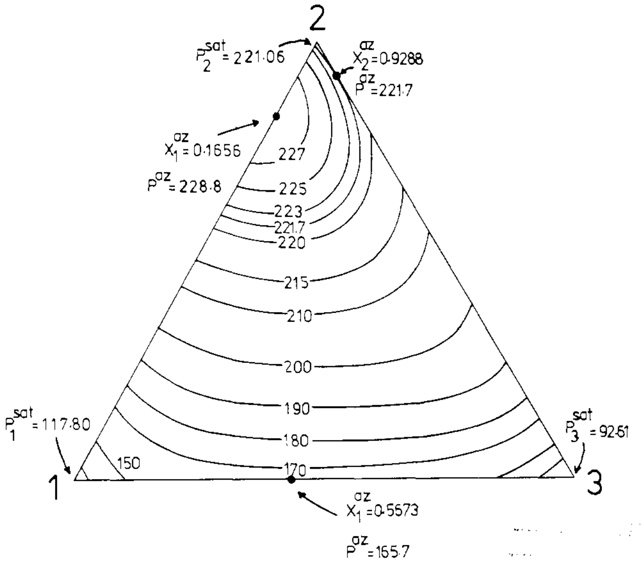

Figure 3. Lines of constant P(mmHg) for the 1,4-dioxane (1)-ethanol (2)-water (3) system at 50 °C.

The ternary data are well fit by the simple Wohl expression.

$$g_{123} = g_{12} + g_{13} + g_{23} + Cx_1x_2x_3 \qquad (2)$$

Correlations for the g_{ij} are provided by eq 1; parameter C is found by regression of just the ternary data.

Second virial coefficients B_{ij} required to account for vapor-phase nonidealities are estimated by the method of Tsonopoulos (11).

Results of the correlations of data for the binary systems, together with all ancillary information, are summarized in Table VI. Correlation of the data for the ternary system, with binary parameters fixed at the values given in Table VI, yields for the ternary parameter the value

$$C = 2.771 \pm 0.009$$

The RMS (root-mean-square) ΔP for the ternary data is 0.041 kPa; the maximum $|\Delta P|$ is 0.068 kPa. A slight improvement in the correlation results if C is made a function of composition:

$$C = 2.411 + 0.500(1 - x_3)$$

This correlation reduces the RMS ΔP to 0.028 kPa and the max $|\Delta P|$ to 0.061 kPa.

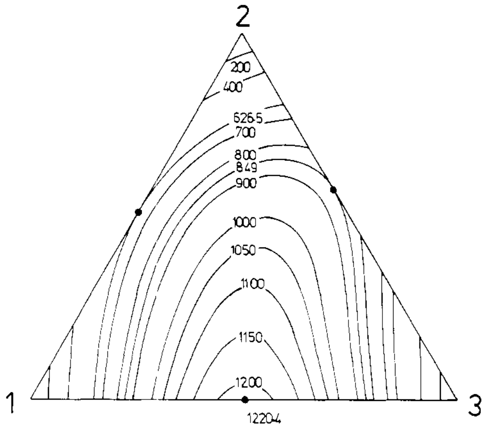

Figure 4. Lines of constant G^E (J/mol) for the 1,4-dioxane (1)–ethanol (2)–water (3) system at 50 °C.

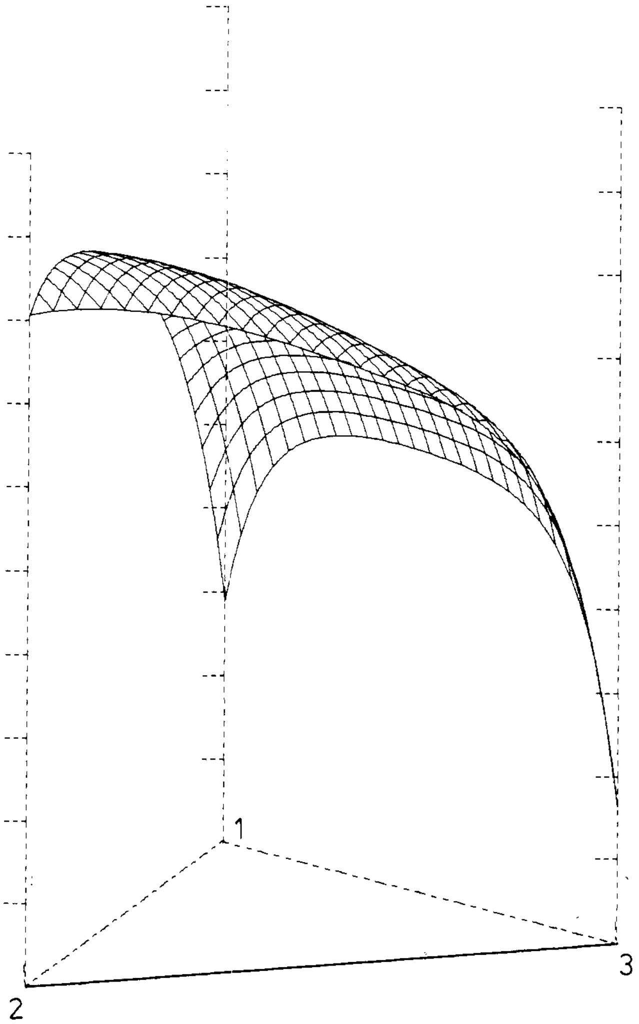

Figure 5. Pictorial view of the P–x surface for the 1,4-dioxane (1)–ethanol (2)–water (3) system at 50 °C.

Discussion

No previous work directly comparable with ours appears in the literature for the ternary system or for the dioxane–ethanol binary. Valent (*12*) reports P–x–y data for the dioxane–water system at 50 °C, and a comparison of his results with ours appears in Figure 1. The pressure and vapor-composition residuals shown there represent the differences between values calculated by our correlation and Valent's experimental values. In these calculations Valent's measured P_i^{sat} values are used, because his value for dioxane differs appreciably from ours. The pressure residuals scatter properly around zero and yield RMS ΔP = 0.088 kPa. The composition residuals show systematic deviations, indicating some thermodynamic inconsistency in Valent's results.

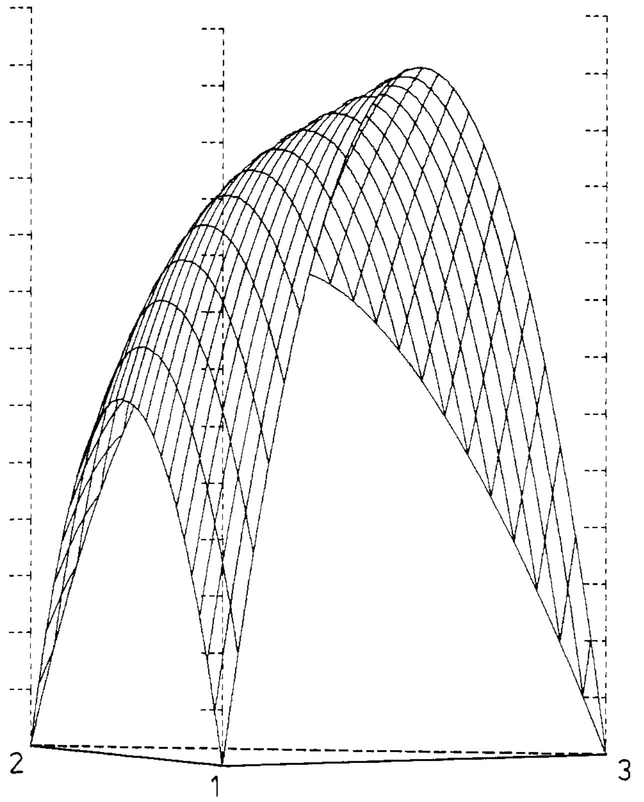

Figure 6. Pictorial view of the G^E–x surface for the 1,4-dioxane (1)–ethanol (2)–water (3) system at 50 °C.

For the ethanol–water system comparisons are made with two sets of published results, those of Pemberton and coworkers (*8*, *10*) and with those of Wilson et al. (*14*). The results of these comparisons are shown in Figure 2, where the plotted residuals are the differences between correlated results of this work and correlated results of the earlier studies. The most significant feature of these plots is the rather large deviation between our results and those of Pemberton at ethanol mole fractions below 0.2. Because of this discrepancy, we repeated the run made for the lower range of ethanol mole fractions. This second run agreed well with the first, and both are included in the data of Table IV. The comparison of our results with those of Wilson et al. shows excellent agreement, with RMS ΔP = 0.031 kPa and max $|\Delta P|$ = 0.049 kPa.

The results of this study are displayed pictorially by Figures 3 through 6. Although each binary system exhibits a maximum-pressure azeotrope, no ternary azeotrope or other singular point appears on the pressure–composition surface.

Glossary

A_{ij}, A_{ji}	parameters in eq 1
B_{ij}	second virial coefficient
C	parameter in eq 2
G^E	excess Gibbs function, liquid phase
g	G^E/RT
P	total pressure
P^{az}	azeotropic pressure
P_i^{sat}	vapor pressure of pure i
R	universal gas constant
T	absolute temperature
V_i^L	molar volume of pure liquid i

x	mole fraction, liquid phase
x^{az}	azeotropic composition
y	mole fraction, vapor phase

Greek Letters

λ	parameter in eq 1
Δ	signifies a difference

Literature Cited

(1) Abbott, M. M., Floess, J. K., Walsh, G. E., Van Ness, H. C., *AIChE J.*, **21**, 72 (1975).
(2) Abbott, M. M., Van Ness, H. C., *AIChE J.*, **21**, 62 (1975).
(3) Ambrose, D., Lawrenson, I. J., *J. Chem. Thermodyn.*, **4**, 755 (1972).
(4) Ambrose, D., Sprake, C. H. S., Townsend, R., *J. Chem. Thermodyn.*, **7**, 185 (1975).
(5) DiElsi, D. P., Patel, R. B., Abbott, M. M., Van Ness, H. C., *J. Chem. Eng. Data*, **23**, 242 (1978).
(6) Gibbs, R. E., Van Ness, H. C., *Ind. Eng. Chem. Fundam.*, **11**, 410 (1972).
(7) Keenan, J. H., Keyes, F. G., Hill, P. G., Moore, J. G., "Steam Tables", Wiley, New York, N.Y., 1969.
(8) Larkin, J. A., Pemberton, R. C., *Natl. Phys. Lab. (U.K.), Rep. Chem.*, 43 (1976).
(9) McGlashan, M. L., Rastogi, R. P., *Trans. Faraday Soc.*, **54**, 496 (1958).
(10) Pemberton, R. C., Mash, C. J., *J. Chem. Thermodyn.*, **10**, 867 (1978).
(11) Tsonopoulos, C., *AIChE J.*, **20**, 263 (1974).
(12) Valent, V. as given in Gmehling, J., Onken, U., "Vapor-Liquid Equilibrium Data Collection. Aqueous-Organic Systems", Vol. I, Part 1, Dechema, Frankfurt, 1977, p 388.
(13) Vinson, G. C., Martin, J. J., *J. Chem. Eng. Data*, **8**, 74 (1963).
(14) Wilson, S. R., Patel, R. B., Abbott, M. M., Van Ness, H. C., *J. Chem. Eng. Data*, preceding paper in this issue.

Received for review October 10, 1978. Accepted January 8, 1979. Partial support (about 30%) for this work came from National Science Foundation Grant No. ENG78-10048, and the remainder from the Department of Chemical and Environmental Engineering, Rensselaer Polytechnic Institute.

Density Estimations for Explosives and Related Compounds Using the Group Additivity Approach

Craig M. Tarver

University of California, Lawrence Livermore Laboratory L-324, Livermore, California 94550

A first-order group additivity approach was used to estimate the densities of 188 explosives and related compounds of very diverse compositions. Of the 173 compounds for which direct comparisons could be made, 40.5% of the estimated densities were within 1% of the measured densities, 33.0% were within 1 to 2%, 16.8% were within 2 to 3%, and 9.8% deviated more than 3% from the measured densities. The average absolute error in density was 0.0191 g/cm^3, and the absolute error in density exceeded 0.05 g/cm^3 for only 14 of the 173 compounds (8.1%). The largest errors occurred for compounds with several bulky highly polar groups in close proximity and for compounds containing groups whose calculated molar volumes were based on density data for a small number of compounds. Inclusion of second-order effects, such as nearest neighbor interactions, phase transitions, and crystalline structure in a second-order group additivity model, appears necessary for accurate density estimations in certain types of compounds.

Introduction

As new families of organic compounds are identified for synthesis as potential high-energy explosives, a technique is required to estimate their steady-state detonation and metal acceleration properties. These estimated detonation parameters can then be compared with those measured for known explosives. Only the new molecules that offer significant advantages over currently used explosives would have to be synthesized and tested for their usefulness as explosives. A synthesis effort guided in this way would have the greatest probability of producing new, more powerful explosive molecules.

The main detonation property that determines the impulse delivered by an explosive is the Chapman–Jouguet (CJ) pressure, P_{CJ}, which is given by

$$P_{CJ} = \rho_0 D^2/(K + 1) \qquad (1)$$

where ρ_0 is the initial density of the explosive, D is the detonation velocity, and K is the adiabatic expansion coefficient of the chemical reaction product gases at the CJ state. Because the detonation velocity and the adiabatic expansion coefficient both increase linearly with the initial density, eq 1 implies that P_{CJ} is proportional to the initial density squared. Measurements of P_{CJ} for various explosives have shown that P_{CJ} is indeed proportional to the square of the initial density. Therefore, to develop more powerful explosives, energetic molecules with very high densities must be identified.

The CJ pressure of an explosive can be calculated to within experimental measurement accuracy by a thermodynamic equilibrium computer code, such as the TIGER code (*3*), or, for explosives containing only C, H, O, and N atoms, by the empirical formula of Kamlet et al. (*10*). These methods require only the molecular formula, the heat for formation, and the initial density of the explosive as input data for a CJ detonation calculation. Hardesty and Kennedy (*9*) recently developed an approximate method of estimating the effective specific energy of an explosive in metal acceleration applications that requires this same input data. The group additivity approach to heat of formation estimation (*1*, *16*) is usually accurate to within ±2 kcal/mol; and, since explosives release 200–500 kcal/mol of energy when detonated, this approach may be confidently used in detonation calculations for hypothetical explosive molecules. Reliable detonation calculations thus require only an accurate method of estimating densities of explosives. This paper presents density estimations for known explosives and related compounds obtained using the group additivity approach.

The prediction of the density of a solid or liquid explosive with no knowledge of its physical properties is difficult; no general method to predict the density of complex organic molecules exists. Three general approaches to density prediction were reviewed: potential function, the theory of close packing for solids, and group additivity. The potential function approach is attractive because it evolves from first principles, and some recent progress (*15*) has been made in its application to large organic molecules. However, as shown by Lee et al. (*14*), the